Sensors & Actuators: B. Chemical 331 (2021) 129423

Contents lists available at ScienceDirect

Sensors and Actuators: B. Chemical

journal homepage: www.elsevier.com/locate/snb

A lightweight, wireless Bluetooth-low-energy neuronal recording system for mice

Shinnosuke Idogawa [a], Koji Yamashita [a], Rioki Sanda [a], Rika Numano [b,c], Kowa Koida [c,d], Takeshi Kawano [a,*]

[a] Department of Electrical and Electronic Information Engineering, Toyohashi University of Technology, Toyohashi, 441-8580, Japan
[b] Department of Applied Chemistry and Life Science, Toyohashi University of Technology, Toyohashi, 441-8580, Japan
[c] Electronics-Inspired Interdisciplinary Research Institute, Toyohashi University of Technology, Toyohashi, 441-8580, Japan
[d] Department of Computer Science and Engineering, Toyohashi University of Technology, Toyohashi, 441-8580, Japan

ARTICLE INFO

Keywords:
Bluetooth low energy
Mouse neuronal recording
Lightweight

ABSTRACT

Electrophysiological recording, which has made significant contributions to the field of neuroscience, can be improved in terms of signal quality, invasiveness, and use of cables. Although wireless recording can meet these requirements, conventional wireless systems are relatively heavy and bulky for use in small animals such as mice. This study developed a low-cost Bluetooth low-energy (BLE)-based wireless neuronal recording system weighing <3.9 g and measuring 15 × 15 × 12 mm^3, with easy assembly, good versatility, and high signal quality for recordings. Both acute and chronic *in vivo* recordings of mice confirm the wireless recording capabilities of the system, with improvements in terms of the power spectral density (PSD) and signal-to-noise ratio (SNR) compared with wired recording. Because of its low weight and compactness, the BLE-based wireless neuronal recording system can be used not only in mice but also in other animals, such as rats and monkeys, thus expanding the application of electrophysiological recordings in neuroscience.

1. Introduction

Electrophysiological recordings are taken by introducing microscale electrodes into the brain tissue of a subject to obtain high-density extracellular recordings of neuronal activity. This technique has made significant contributions to fundamental neuroscience research and medical applications, including the brain–machine interface (BMI) technology. However, electrophysiological recordings require a high recording quality in terms of the spatiotemporal resolution, signal-to-noise ratio (SNR), and invasiveness to minimize tissue damage and enable stable, long-period recordings under electrode implantation. Micro-/nanoscale fabrication technologies meet these requirements, including numerous commercially available microelectrode devices [1–4] with a typical impedance of >100 kΩ at 1 kHz. However, common issues with microelectrode devices are the external noise and interfering signals, which are easily coupled with the recording cables between the recording electrode and the first-stage amplifier, thereby degrading the recording quality (neuronal signals <500 μV [5–7]. In addition, when applied to freely moving animals, the signal cable causes further issues regarding the noise level associated with the cable's motion and inhibition of the animal's behavior [8,9].

A wireless recording technology can overcome these issues [8–14]. When applied to small animals, a wireless recording system should be lightweight and compact. Wireless neural recordings of mice and rats using a commercially available system have been reported [8]. The system comprises a neuronal recording chip (15 channels) with a radio frequency (RF) circuit for the signal transmitter. The integrated system excluding the battery weighed 4.5 g and measured 22 × 22 mm^2. The "Hermes" family of wireless recording systems are quite compact [15,16]. The latest chip from Hermes comprises a neuronal recording chip (96 channels) with an on-chip digitizer and an off-chip ultra-wide-band (UWB) transmitter. The chip, measuring 5 × 5 mm^2, was fabricated using the complementary-metal-oxide-semiconductor (CMOS) technology with a custom circuit design [17]. Since wireless recording systems are based on their own custom technologies, they do not meet the high versatility and low-cost requirements. To this end, a low-cost, highly versatile 2.4 GHz Bluetooth radio system-on-a-chip (SoC) has been proposed that allows customizing the protocol [14]. In addition,

* Corresponding author at: Department of Electrical and Electronic Information Engineering, Toyohashi University of Technology, 1-1 Hibarigaoka Tempaku-cho, Toyohashi, Aichi, 441-8580, Japan.
E-mail address: kawano@ee.tut.ac.jp (T. Kawano).

https://doi.org/10.1016/j.snb.2020.129423
Received 19 August 2020; Received in revised form 18 November 2020; Accepted 24 December 2020
Available online 8 January 2021

Bluetooth enables bidirectional wireless communication up to 5 m from the subject. However, conventional Bluetooth-based wireless neuronal recording systems are typically bulky (>22 × 30 mm^2 [14]) and heavy (>12 g [14]), particularly when applied to small animals. For use in mice, the total weight of the system, including the battery, should be <5 g, which is ~15 % of a mouse's weight (*e.g.*, a two-week-old C57BL/6 mouse weighs 33 g). Therefore, the entire system should be miniaturized for neuronal recordings in freely moving mice.

In this study, we developed a Bluetooth low-energy (BLE)-based wireless recording system for use in mice. The system weighs <3.9 g and measures 15 × 15 × 12 mm^3 (Fig. 1a). To confirm its neuronal recording capability, we connected it to our silicon growth technology-based

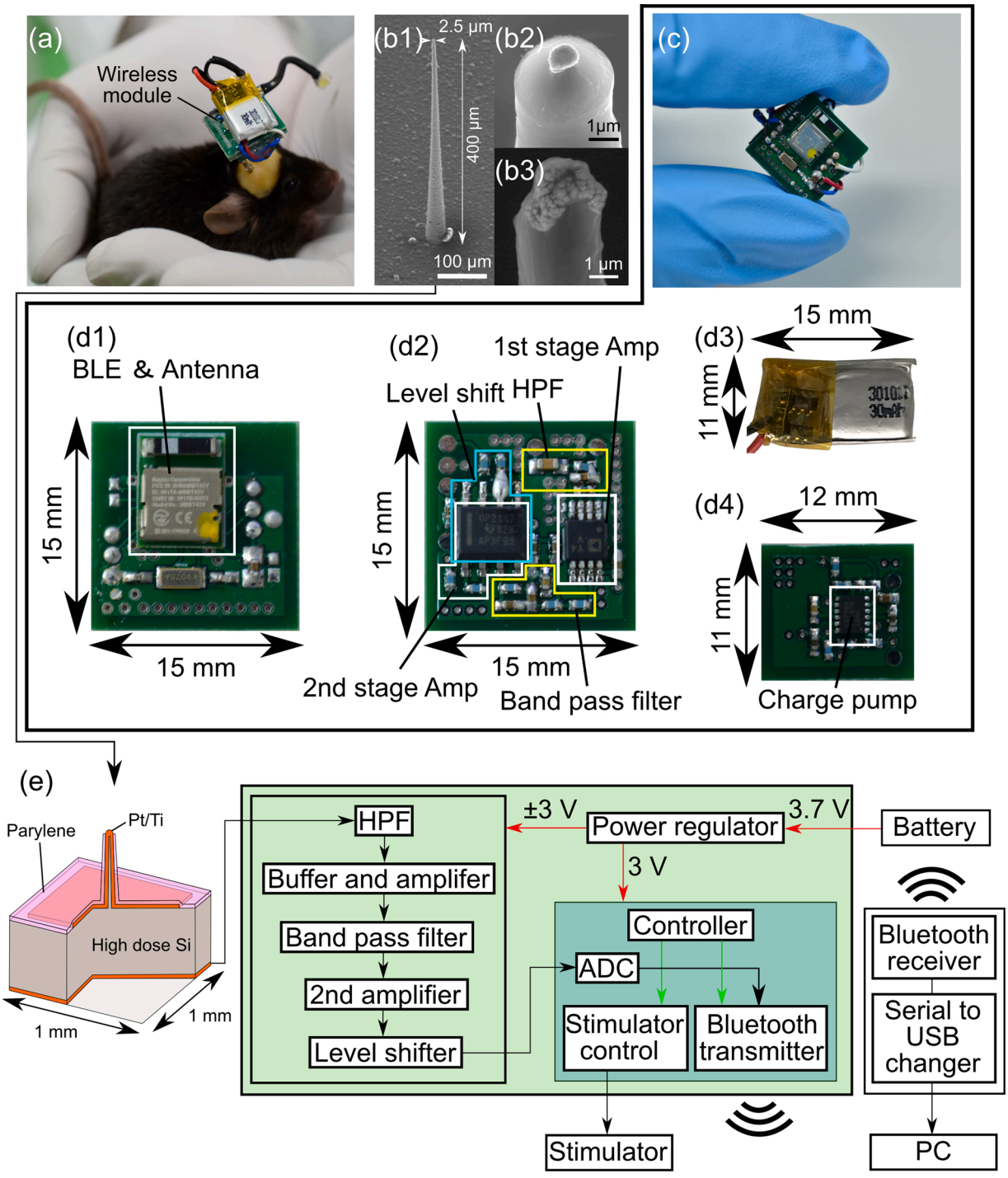

Fig. 1. Lightweight, small-scale, BLE-based wireless neuronal recording system for mice. (a) Photograph of a mouse with a head-mounted wireless neuronal recording system for neuronal signal transmission. (b) SEM images of a silicon growth technology-based microneedle electrode: (b1) overall electrode with 400 µm length and <5 µm tip diameter, and enlarged images of the tip section of the microneedle electrode (b2) before and (b3) after electroplating with platinum black. (c) Photograph of the wireless neuronal recording system with a power regulator module and amplifier module at the back. (d) Photographs of wireless neuronal recording system components: (d1) Bluetooth transmitter module, (d2) amplifier circuit module, (d3) battery, and (d4) power regulation circuit module. (e) Block diagram of the wireless neuronal recording system, comprising the electrode module, wireless system module, battery module, and receiver. BLE, Bluetooth low energy; SEM, scanning electron microscopy.

single-channel microneedle electrode (<5 μm in diameter; >600 kΩ impedance at 1 kHz) [18]. The recording capability was evaluated by taking acute and chronic neuronal recordings of mice, and the signal quality was compared with that of a conventional wired recording system. We also performed wireless neuronal recordings in freely moving mice.

2. Materials and methods

2.1. Device fabrication

We used a 5 μm-diameter microneedle electrode [19] for low-invasive electrophysiological neuronal recordings of mice [18] and rats [5]. The 400 μm-long microneedle was located at the center of a 1 × 1 mm^2, 525 μm-thick silicon block (Fig. 1b1). The microneedle was metalized with platinum and then insulated with parylene-C (~1 μm thick), except for the tip (Fig. 1b2). The tip diameter of the microneedle electrode after plating a low impedance material of platinum black [5,18] was 3 μm (Fig. 1b3), and the electrode device weighed 0.067 g. Owing to the mechanical properties of the silicon needle, the microneedle electrode has sufficient mechanical strength for tissue penetration [18,20] (Supplementary Information).

Fig. 1c shows our BLE-based wireless neuronal recording system (weighing <3.9 g including the battery; size: 15 × 15 × 12 mm^3, Table 1). The system comprises a Bluetooth transmitter module (Fig. 1d1) connected to an amplifier circuit module (Fig. 1d2) to measure the neuronal activity (<500 μV). The amplifier helped eliminating the drifts and offsets accosiated with the interfacial electrical properties between the microneedle electrode (platinum black) and the saline solution. The amplifier circuit module, which had a higher input impedance (200 GΩ) than the microneedle electrode, amplified the recorded signals to a voltage level that could be detected using an analog–digital converter (ADC). Furthermore, it was necessary to remove aliasing noise associated with the sampling theorem and radiofrequency interference (RFI) noise during Bluetooth communication. A 3.7 V lithium battery (weighing 0.85 g, Fig. 1d3) supplied power to the BLE-based wireless neuronal recording system, and the power regulation circuit module (LM27762; Texas Instruments Inc., U.S.A.) (Fig. 1d4) provided a supply of ±3 V, one for the analog circuit and the other for the digital circuit (Bluetooth transmitter module).

Fig. 1e shows a block diagram of our BLE-based wireless neuronal recording system. We designed a high-pass filter (HPF) with a cut-off frequency of 1.59 Hz to eliminate the metal (platinum black)–electrolyte (saline) interfacial characteristics-induced voltage drift of the electrode. Another HPF with a cut-off frequency of 1.69 Hz was used to eliminate the offset of the amplifier. These filter configurations allowed acquiring slow signal components corresponding to the delta (1.5–4 Hz) and theta (4–10 Hz) bands [21]. A 59 dB first-stage operational amplifier (AD8422; Analog Devices, Inc., U.S.A.) (input impedance of 200 GΩ) was used to amplify the neuronal signals from microvolts to millivolts. This amplifier also played a role in impedance conversion. A second-order low-pass filter (LPF) with a cut-off frequency of 3 kHz was also used. This cut-off frequency helps reduce aliasing to the ADC, allowing to acquire narrow-band signals of unit activity (*e.g.*, > 500 Hz) under the Nyquist frequency. The second amplifier (OPA2187; Texas Instruments, Inc., U.S.A.) gain stage produced an additional gain of 15.1 dB. These signals were then set to a positive input for the ADC of the BLE chip (MDBT42 V; Raytac Corporation, Taiwan) using a level shifter.

Table 1
Specifications of a Bluetooth low-energy neuronal recording system developed for mice.

Battery life	2.5 h
Transmit range	5 m
Transmission frequency	2.4 GHz ISM
Total weight	3.9 g (with battery)
Total size	15 × 15 × 12 mm^3
Power consumption	28.6 mW
Sampling rate	10 k samples/s
Number of channels	1 ch

The ADC was a 12-bit successive approximation register (SAR), and the neuronal activities at a frequency of approximately 1 kHz were acquired with a sampling rate of 10k samples/s, although the maximum sampling rate of the ADC is 200k samples/s. Digital data from the ADC were converted to hexadecimal American Standard Code for Information Interchange (ASCII) code and then transmitted through the BLE chip antenna.

The data were transferred after completing the recording. The transmitted data were received by a BLE receiver module (nRF52840 DK; Nordic Semiconductor ASA, Norway) with a serial-to-USB converter (MIKROE-483; MikroElektronika, Serbia) and then processed on a personal computer (PC) with a logger software that supports the serial communication protocol. The data were converted to a comma-separated-value (CSV) file format and then analyzed using MATLAB (The MathWorks, Inc. U.S.A.). To receive the data on a smartphone, the data can be converted to the CSV file format within the smartphone using a development application [nRF connect or nRF UART (Nordic Semiconductor ASA, Norway)]. For the physical stimulation of the mouse, we used general-purpose input/output (GPIO) ports of the Bluetooth transmitter module to control either the somatosensory or visual stimulator.

By adding the cost of each individual component, we estimated the total cost (USD-United States Dollar) of the wireless system to be $79.9 [Bluetooth transmitter module ($11.1), amplifier circuit module ($10.4), power regulation circuit module ($5.0), and Bluetooth receiver module (with a serial-to-USB converter) ($53.4)].

2.2. Acute in vivo recordings

We confirmed the neuronal recording capability of our system by taking *in vivo* neuronal recordings of mice. We anesthetized mice (n = 7, body weight: 23.7–40.7 g) using an intraperitoneal injection of urethane solution (0.5 % chlorprothixene [0.10 mL/10 g] and urethane [0.05 mL/10 g]). The head of each mouse was fixed using a stereotaxic apparatus (SR-50; Narishige, Tokyo, Japan), and parts of the cranium and dura mater were removed (~2 mm diameter) before placing microneedle electrode over the cerebral cortex and penetrating them at the primary somatosensory field (S1B) (−1 mm posterior and 3 mm lateral to the bregma) on the right hemisphere *via* the fenestrae in the cranium and dura mater. The recording site of the microneedle was stereotaxically defined by the brain atlas [22].

The microneedle electrode was attached to a micromanipulator (MO-10; Narishige) to control the microneedle placement. The complete penetration of the microneedle into the brain tissue was confirmed using an optical microscope. To record the somatosensory responses, we penetrated the microneedle electrode into the S1B. As a signal reference electrode, we drilled a stainless-steel screw (1 mm diameter) (AM-1.4-2, Unique Medial Co., Ltd., Japan) into the skull over the visual cortex (V1) (−4 mm posterior and 2.5 mm lateral to the bregma) on the left hemisphere. During the recording, we physically stimulated specific whiskers using an electromagnetic vibrator (custom-built) driven by electrical pulses applied for a duration of 1 ms at 3 s intervals to activate the neurons at S1B, while keeping the cortical surface wet by adding saline in a dropwise manner. The whisker stimulation was controlled using a wireless recording system (GPIO port in the Bluetooth transmitter module). The distance between the Bluetooth transmit module and the BLE receiver module was approximately 2 m.

All the experimental procedures involving the mice were approved by the Committee for the Use of Animals at Toyohashi University of Technology, Japan. All the animal care procedures were conducted in accordance with the Standards Relating to the Care and Management of Experimental Animals (Notification No. 6, 27 March 1980, of the Prime

Minister's Office of Japan).

2.3. Chronic in vivo recordings

Chronic recordings were taken from needle-electrode-implanted mice, and the signal qualities of the wired and wireless recordings were compared. For the electrode implantation, we used mice (n = 2, body weight: 31.8–33.2 g) anesthetized using isoflurane. After the head of the mouse was fixed with a stereotaxic apparatus, similar to the technique employed for the acute recording, parts of the cranium and dura mater of the mouse were removed before placing the needle electrode over the cerebral cortex and penetrated at V1 (−4 mm posterior and 2.5 mm lateral to the bregma) on the right hemisphere *via* the fenestrae in the cranium and dura mater. As a signal reference electrode, a metal pin (gold, 1 mm diameter) was drilled into the skull over the S1B (−1 mm posterior and 3 mm lateral to the bregma) on the left hemisphere. To protect the brain surface, a gelatin sponge was placed over the surface, and the needle electrode was fixed onto the skull with dental cement. For visual stimulation, we used a white light-emitting diode (LED), located 15 mm from the mouse's left eye with an angle of 45° and illuminated for 0.5 s at 3 s intervals to record the visual responses.

2.4. Wired neuronal recording system for signal comparison

To compare the signal qualities of the wireless recording system with that of the wired recording system, each recording was separately performed within one hour using the same needle-electrode-implanted mouse (n = 2). The corresponding PSD and SNR values were then evaluated. We used a commercial neurophysiology system for the wired recording. In the signal acquisition and processing procedure, the signals recorded using the microneedle electrode were differentially amplified (ZC64, Tucker-Davis Technologies, 1×10^{14} Ω input impedance) with filters (0.35 Hz for low-cut-off and 7.5 kHz for high-cut-off). Following signal amplification, the signals were routed to a preamplifier/digitizer (PZ2, Tucker-Davis Technologies) and a digital signal processing module (RZ2, Tucker-Davis Technologies). The digital data were then stored on a hard disk in a Windows PC with a sampling frequency of 25 kHz. During the neuronal recording, a LED was used to apply visual stimuli to the mouse. The PSDs of each recording system were calculated by applying a fast Fourier transform (FFT) to each trial and then averaging these trials. The SNR was defined as the peak-to-peak amplitude of unit activities of the mean waveform 5–50 ms after stimulus onset, divided by the root-mean-square signals 0–50 ms before stimulus onset.

2.5. In vivo recording in a freely moving mouse

We demonstrated wireless neuronal recording in a freely moving mouse using the same BLE-based wireless neuronal recording system as that used for the acute and chronic neuronal recordings. In addition, we used the same needle-electrode-implanted mouse (visual cortex, V1) as the one employed in the chronic *in vivo* recordings. We did not use chlorprothixene, as it inhibits spontaneous activity and movement of the mouse. The mouse's eye was stimulated using the LED, which was connected to our wireless system, and the illuminations were controlled using the Bluetooth transmitter module.

The stimulation parameters of the LED were the same as those used for the chronic *in vivo* recordings (an illumination duration of 0.5 s at 3 s intervals). During the recording, the mouse was placed in a mouse cage having dimensions of $20 \times 31 \times 11 cm^3$. The distance between the Bluetooth transmitter module (mouse's head) and the BLE receiver module was ~1.5 m.

3. Results

3.1. BLE-based wireless neuronal recording system

First, we characterized the electrical impedances of the microneedle–electrode device, the amplifier gains, and the noise spectrum of the fabricated BLE-based wireless recording system, to demonstrate the capability of the wireless recording system in mice. Fig. 2a shows the impedance magnitudes of the used microneedle electrode before and

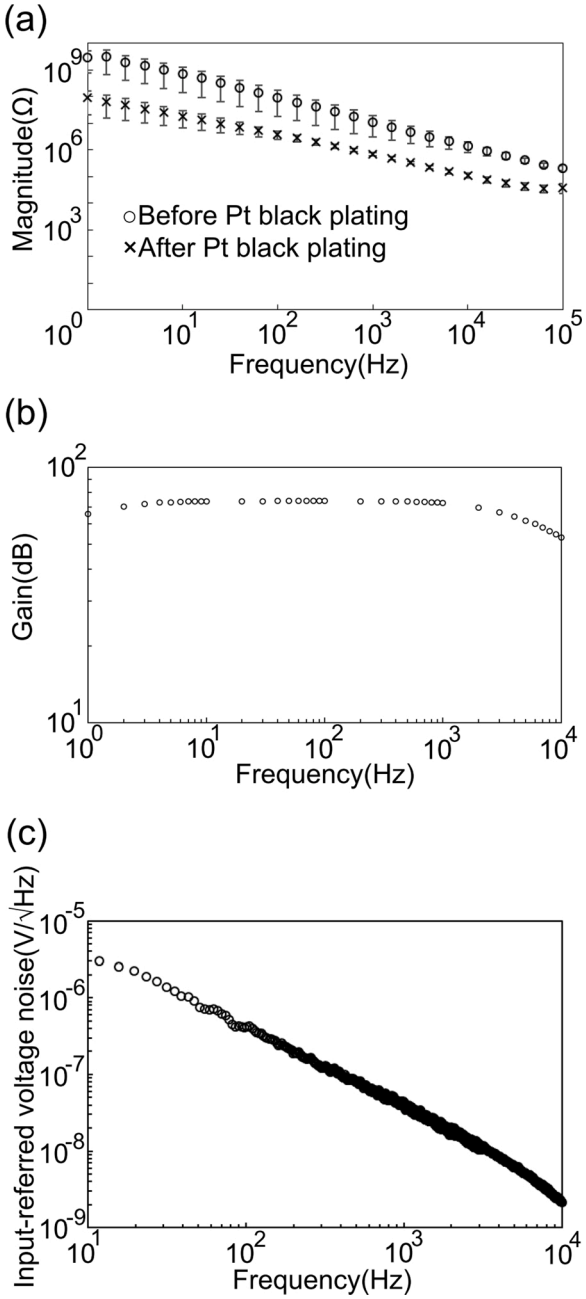

Fig. 2. Electrical properties of our BLE-based wireless neuronal recording system equipped with needle electrode. (a) Impedance magnitudes of the microneedle electrode before (circles) and after (crosses) electroplating with platinum black, measured in a phosphate buffered saline in the frequency range of 1 Hz – 100 kHz. The averages and standard deviations are taken from three samples for each curve. (b) Measured transfer function of the system. The midband gain is 72 dB, a single roll-off occurred at 3 kHz, and a low-frequency roll-off occurred at 1.6 Hz. (c) Measured input-referred voltage noise spectrum of the system. BLE, Bluetooth low energy.

after electroplating with platinum black, measured in a phosphate buffered saline in the frequency range of 1 Hz – 100 kHz. Before the platinum black plating, the impedance associated with the electrolyte–metal interfacial properties was 11.2 ± 8.0 [mean ± standard deviation (SD)] MΩ, which was reduced to 690 ± 86 (mean ± SD) kΩ by plating with platinum black (nano-scale porous of platinum) with increased effective surface area [18].

Fig. 2b shows the transfer function of our BLE-based wireless neuronal recording system, while applying test signals in the form of 100 μV peak-to-peak sinusoidal waves at frequencies swept from 1 Hz to 10 kHz. The measured gains ranged from 53.1–73.8 dB (72.6 dB at 1 kHz). A cut-off frequency >3 kHz enabled the recording of not only the wideband signals of the local field potentials (*e.g.*, <500 Hz) but also the narrow-band signals of unit activity (*e.g.*, >500 Hz). The unit activity of the neurons exhibited low voltage amplitudes, as low as 50 μV, which could be amplified to a sufficient voltage level for the ADC using the amplifier gains.

The input-referred noise spectrum of the fabricated system was obtained by measuring the output noise using a spectrum analyzer and then dividing the noise by the amplifier gain. Fig. 2c shows the measured input-referred noise spectrum of our system. A noise level of <1 μV in the frequency range of 50 Hz – 10 kHz was acceptable because of the typical extracellular neuronal background noise level of 5–10 μVrms [18,23,24] and neuronal activity potentials >100 μV for the local field potential (LFP) and > 50 μV for unit activity.

3.2. *In vivo* neuronal signal recordings

3.2.1. *Acute recordings*

Fig. 3a–c shows the wireless neuronal acute recordings from the S1B of mice *in vivo*. Fig. 3d1 shows the recorded LFP (third Butterworth filter [80–500 Hz]). The LFPs emerged in response to the whisker stimuli with a latency of ~20 ms. The amplitude of the mean waveform taken from 100 trials was ~360 μV (blue waveform, Fig. 3d1). Fig. 3d2 shows the recorded single trial of the unit activity band potential (second Butterworth filter [500–3000 Hz]). Fig. 3d3 and d4 show the raster plots and the peristimulus time histograms (PSTHs), respectively, for the 100 trials. Signal spikes were detected based on the triggering of thresholds for four standard deviations (SDs, σ) of the mean signal during 10 – 300 ms before stimulation onset. A further analysis suggested that these recorded spikes can be categorized into multiunit activity. In addition, these LFP and unit activity signal waveforms were similar to those of the signals recorded by conventional tungsten electrodes and our previous micro-/nanoscale needle electrode devices [5,25]. These sensory responses appeared ~20 ms following whisker stimulation and were consistent with the reported latency in the whisker stimulation of mice [18]. Therefore, the signals recorded by our BLE-based wireless neuronal recording system were neurophysiological responses evoked by whisker stimuli.

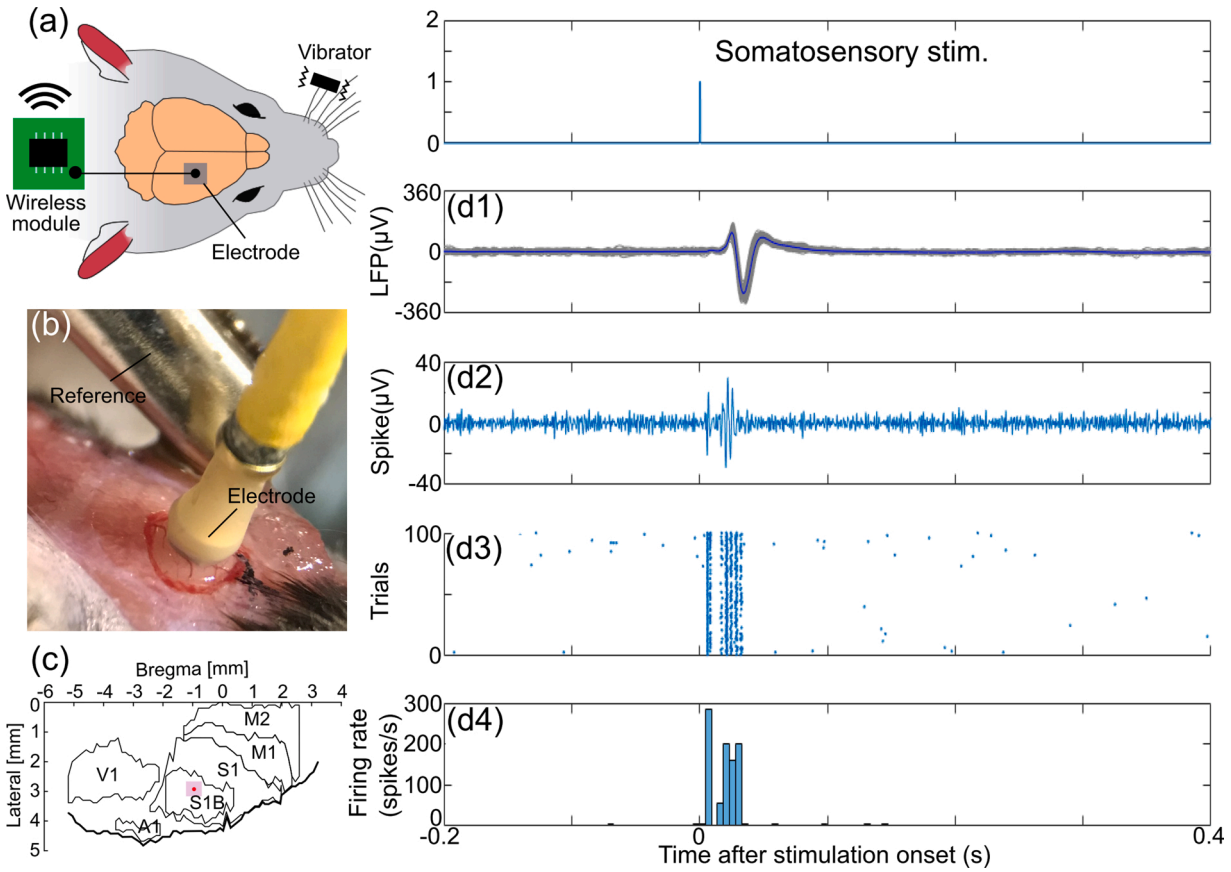

Fig. 3. Acute *in vivo* neuronal recording from the cortex of a mouse using our BLE-based wireless neuronal recording system. (a, b) Schematic and photograph of the neuronal recording, showing the electrode module placed over the cortex. The microneedle electrode is connected to a wireless system module with a 6 cm-long cable. The mouse's whiskers are physically stimulated using an electromagnetic vibrator. (c) Schematic showing the position of the microneedle electrode, which penetrates the primary somatosensory cortex barrel field (S1B). (d) Recorded signals using the wireless neuronal recording system: (d1) LFP waveform signals using a band-pass filter (third Butterworth filter [80–500 Hz]), single trial (gray) and average (blue), (d2) single-trial signal from recordings for 100 trials using a band-pass filter (second Butterworth filter [500–3000 Hz]), and (d3, d4) raster plots and PSTHs taken from the signals (500–3000 Hz) using detection amplitude thresholds of 4σ of the mean signal during 10–300 ms before stimulation onset. BLE, Bluetooth low energy; PSTH, peristimulus time histogram (For interpretation of the references to colour in this figure legend, the reader is referred to the web version of this article).

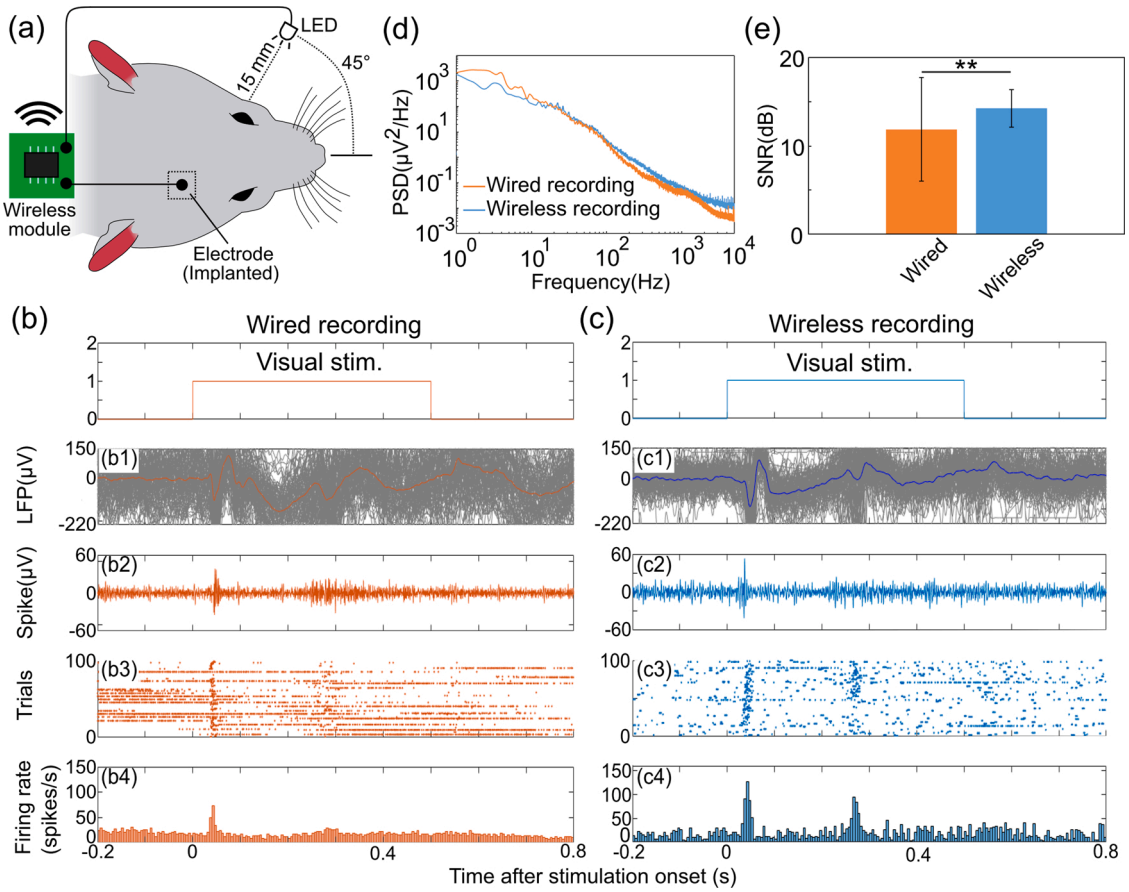

Fig. 4. Chronic *in vivo* neuronal recording from the cortex of a mouse using a wired recording system and our BLE-based wireless neuronal recording system. (a) Schematic of the recording, showing the system connected to a microneedle electrode implanted at the primary visual cortex (V1) of the mouse. The mouse is stimulated using an LED to record visual responses. (b) Recorded signals using the wired recording system: (b1) waveform signals using a band-pass filter (third Butterworth filter [80–500 Hz]), (b2) single trial signal from recordings for 100 trials using a band-pass filter (second Butterworth filter [500–2000 Hz]), and (b3, b4) raster plots and PSTHs taken from the signals (500–2000 Hz) using detection amplitude thresholds of 4σ of the mean signal during 10–300 ms before stimulation onset. (c) Recorded signals using the wireless recording system: (c1) waveform signals using a band-pass filter (third Butterworth filter [80–500 Hz]), (c2) single-trial signal from recordings for 100 trials using a band-pass filter (second Butterworth filter [500–2000 Hz]), and (c3, c4) raster plots and PSTHs taken from the signals (500–2000 Hz) using detection amplitude thresholds of 4σ of the mean signal during 10–300 ms before stimulation onset. (d) Comparison of PSDs between wireless and wired recordings using the same electrode module and mouse but with varying recording cable length. (e) Comparison of SNRs between wireless and wired recordings using the same electrode module and mouse, calculated with signals obtained after band-pass filtering (second Butterworth filter [500–2000 Hz]). The averages and SDs are taken from 100 samples. Asterisk denotes significant difference in the SNR; double: $p < 0.01$ (n = 100 trials, Welch *t*-test). BLE, Bluetooth low energy; LED, light-emitting diode; PSTH, peristimulus time histogram; PSD, power spectral density; SNR, signal-to-noise ratio; SD, standard deviation.

3.2.2. *Chronic in vivo recording*

We performed chronic *in vivo* recording of the same electrode-implanted mouse using a wired recording system (commercial neurophysiology system, TDT) and the fabricated wireless system, and the signal qualities of the two recording systems were compared. Fig. 4a shows a schematic of the chronic recordings taken from V1 of the mouse. Fig. 4b shows the recorded data using the wired recording system (TDT). Fig. 4b1 shows the recorded LFP (third Butterworth filter [80–500 Hz]). The LFPs emerged in response to visual stimuli with a latency of ~40 ms. Their amplitude was ~220 μV for the 100 trials. Fig. 4b2 shows the unit activity band potential (second Butterworth filter [500–2000 Hz]). Fig. 4b3 and Fig. 4b4 show the raster plots and PSTHs, respectively, for the 100 trials. Signal spikes were detected based on the triggering of the same thresholds for 4σ of the mean signal in the period of 10–300 ms before the stimulation onset.

Fig. 4c shows the recorded data using the fabricated wireless recording system. Similar to the wired recording, LFPs emerged in response to visual stimuli with a latency of ~40 ms, as shown in the recorded LFP in Fig. 4c1 (third Butterworth filter [80–500 Hz]). Their amplitude was ~220 μV for the 100 trials. Fig. 4c2 shows the unit activity band potential (second Butterworth filter [500–2000 Hz]). Fig. 4c3 and Fig. 4c4 show the raster plots and PSTHs, respectively, for the 100 trials. Signal spikes were detected based on the triggering of the same thresholds for 4σ of the mean signal in the period of 10–300 ms before stimulation onset. In the PSTHs (Fig. 4c4), two types of responses can be confirmed, *i.e.*, at ~40 and ~280 ms after the stimulation, representing fast and slow responses to the visual stimulation, respectively [26,27].

The PSD was calculated by applying a fast Fourier transform (FFT) to each trial and then averaging the trials (Fig. 4d). Our wireless system showed lower PSDs compared to the wired recordings at frequencies <20 Hz. This can be attributed to the shorter length of the recording cable (~6 cm) connecting the microneedle electrode and the first-stage amplifier of our system.

Fig. 4e shows a comparison of the SNRs calculated from the results of the unit activity band potentials taken from the chronic wireless and wired recordings (TDT). The SNR of our system was 14.3 ± 2.1 (mean ± SD) dB, which was higher than that of the wired recordings [11.9 ± 5.9 (mean ± SD) dB] ($p < 0.01$, n = 100 trials, Welch *t*-test). This can be attributed to the reduction in the cable-induced noise without significant voltage attenuation of the signals by the shorter cable of our system compared to the wired system. We also confirmed a reduction in the SNR

fluctuation as SD in the wireless recordings, indicating that our BLE-based wireless neuronal recording system improved the signal quality of the neuronal recording.

3.2.3. *In vivo recording in a freely moving mouse*

Fig. 5a shows a photograph of the wireless neuronal recording of a freely moving mouse with a head-mounted system. During the recording, we did not observe any disturbance in the behavior of the mouse due to our wireless system. Fig. 5b1 shows the recorded LFP (third Butterworth filter [80–500 Hz]). The LFPs emerged in response to visual stimuli with a latency of ~40 ms. Their amplitude was ~180 μV for the 100 trials. Fig. 5b2 shows a typical single trial of the unit activity band potential (second Butterworth filter [500–2000 Hz]) for the 100 trials. Fig. 5b3 and b4 show the raster plots and PSTHs, respectively, for the 100 trials. Signal spikes were detected based on the triggering of the thresholds for 3σ of the mean signal in the period of 10–300 ms before stimulation onset (no significance in the PSTHs with 4σ).

The unit activity band potential consisted of not only light stimuli-evoked neuronal activity observed at a latency of ~40 ms (Fig. 5c shows superimposed waveforms of spikes detected with 3σ) but also others observed at a latency of >200 ms (purple colored in Fig. 5b4), though light-evoked LFPs were continuously recorded. The other signals observed at the unit activity band were probably due to the light stimulation-induced series of the responses, including the mouse's shivering (electromyogram [EMG]) and spontaneous activities, which were not observed in the chronic recordings without injecting chlorprothixene (Fig. 4b2–b4, c2–c4). This leads to that reducing the light intensity during the visual stimulation can help eliminate the other event-induced signals (>200 ms, purple colored in Fig. 5b4).

4. Discussion

We developed a lightweight, small-scale BLE-based wireless neuronal recording system for use in mice. A reduction in the weight, including of the battery, is essential for use in small animals such as mice. Our system weighs <3.9 g, with a 3.0 g wireless module and a 0.85 g battery module, and it measures 15 × 15 × 12 mm^3. However, the system can be further miniaturized, for example, by using a molding material with a low-density and lightweight device substrate, such as a thin, flexible polyimide material. Table 2 summarizes the features of our

Table 2
Comparison of our system feature with those of other wireless recording systems.

	BLE-neuronal recording system (This work)	PennBMBI [28]	WAND [14]	TBSI [8]
Total size	15 × 15 × 12 mm^3	56 × 36 × 13 mm^3	36 × 33 × 15 mm^3	22 × 22 × 22 mm^3
Total weight	3.9 g (with battery)	–	17.95 g	4.5 g
Power consumption	28.6 mW	290 mW	–	–
Transmission frequency	2.4 GHz (Bluetooth)	2.4 GHz	2.4 GHz (Bluetooth)	3.05 GHz
Transmit range	5 m	–	–	–
Number of channels	1 ch	4 ch	128 ch	15 ch
Sampling rate	10 k samples/s	21 k samples/s	1 k samples/s	–
ADC resolution	12 bits	12 bits	15 bits	–
Battery life	2.5 h	–	11.3 h	6 h

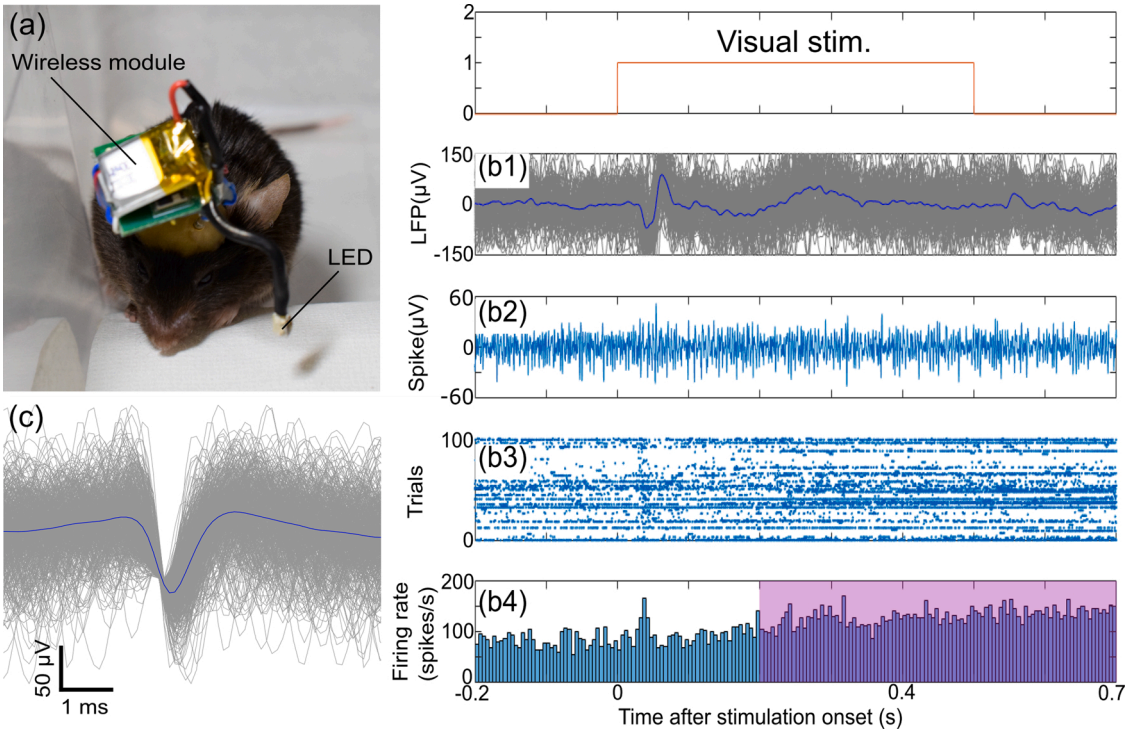

Fig. 5. *In vivo* neuronal recording of a freely moving mouse. (a) Photograph of the recording, showing a mouse with a head-mounted wireless neuronal recording system connected to a microneedle electrode, which penetrates the primary visual cortex (V1). The mouse's eye is stimulated using an LED connected to the system, and the illuminations are controlled using the Bluetooth module. (b1–b4) Signals recorded from the freely moving mouse using the BLE-based wireless neuronal recording system: (b1) waveform signals obtained using a band-pass filter (third Butterworth filter [80–500 Hz]), (b2) single-trial signal from recordings for 100 trials using a band-pass filter (second Butterworth filter [500–2000 Hz]), and (b3, b4) raster plots and PSTHs taken from the signals (500–2000 Hz) using detection amplitude thresholds of 3σ of the mean signal during 10–300 ms before stimulation onset. (c) Superimposed waveforms of spikes 10–60 ms after stimulus onset, detected with 3σ. BLE, Bluetooth low energy; LED, light-emitting diode; PSTH, peristimulus time histogram.

wireless recording system in comparison with those of recently published wireless recording systems. For the neuronal recording of mice, we designed a system with a total weight of 3.9 g, which should be less than ~15 % of a mouse's weight [9] (*e.g.*, <5 g system weight for 33 g two-week-old C57BL/6 mice). Although PennBMBI [28], WAND [14], and TBSI [8] can be used for neuronal recordings with a large number of recording channels, these systems are too bulky to be used in mice. We designed our wireless system with small dimensions of 15 × 15 × 12 mm^3, which is an acceptable size for not only mice but also other small animals, including rats, allowing for their natural movements and behaviors.

Our system architecture allows multichannel wireless recording, though we demonstrated only single-channel recording *via* a microneedle electrode. The ADC of the Bluetooth module has six channels, and each channel can be sampled at >10k samples/s (30k samples/s, which is the maximum sampling rate). It is also possible to mount an analog multiplexer (MAX4691; Maxim Integrated, U.S.A.) and extend the number of recording channels to 16. The multiplexer can be controlled by the same Bluetooth transmit module (BLE chip, MDBT42 V) (Supplementary Information, Table S1). Multichannel wireless recording based on our system architecture can be achieved by increasing the number of channels and each sampling frequency, which will be investigated in the future.

Our system transmits digitized recorded data to the receiver for each trial, and the received data are analyzed offline on a PC. However, a real-time recording of the neuronal signals is necessary for some medical applications such as prosthetic control. Real-time wireless recording can also be performed using another BLE chip BC57E687C (Qualcomm, San Diego, CA, USA), which has a two-channel ADC, where each channel is sampled at 44.1k samples/s and converted to a transmission analog signal in real time. Moreover, to record the evoked responses with a latency < 300 ms by either whiskers or visual stimulations, we used the BLE transmitter with a recording period < 1.5 s; however, this will be extended by reprograming the system.

Our silicon growth technology-based low-invasive microneedle electrode has a microneedle electrode–saline interfacial impedance of 690 kΩ at 1 kHz. Common issues with microelectrode devices with impedance >100 kΩ at 1 kHz are external noise and interfering signals, which can be eliminated by a wireless system. Neuronal recordings must not contain noise sources, including noise coupling with respect to the recording cable, motions of the cable and the animal, and EMG signals generated by the muscles. The EMG signals have a frequency range of 0–500 Hz. The PSD results indicate that wireless recording can help reduce the external noise and interfering signals during chronic recording. In the frequency range of 0.1–5 kHz, the PSD spectrum indicates that wireless recording shows a higher PSD than wired recording. This can be attributed to the impedance (>600 kΩ at 1 kHz) and parasitic impedances of the electrode associated with the longer cable (~30 cm) used in wired recording, where the impedance set induces a voltage divider and results in voltage attenuation in the frequency range [5,29]. Eliminating the recording cable-induced voltage divider in the wired recording system can improve the SNR at the unit activity band. Consequently, the signal quality of neuronal recording using a high-impedance microelectrode can be improved owing to the short recording cable connecting the microelectrode and the first-stage amplifier in a wireless neuronal recording system. To discuss the signal quality, a stable positioning of the implanted electrode (tip section of the needle as the recording site) should be evaluated. The electrode (tip section) may slightly deviate not only because of the fluidity of the brain, but also because of the pulsation of the tissue, though the implanted needle-electrode device was fixed to the skull using dental cement. To define the electrode position within the tissue, candidates include a marking method and immunohistochemical evaluation [5], the investigation of which is ongoing.

5. Conclusion

We developed a < 3.9 g, 15 × 15 × 12 mm^3 BLE-based wireless neuronal recording system for mice. The neuronal recording capability of the system was confirmed by taking acute and chronic recordings *in vivo*, along with wireless neuronal recording of freely moving mice. Because of the low weight and compactness of the system, it does not disrupt animal movements. Since the transmitter uses BLE technology, its advantages include data acquisition using inexpensive devices, such as a PC and a smartphone, doing away with conventional large, expensive recording systems. In addition, there is no significant difference in the recorded data between wireless and conventional wired systems. This makes our highly versatile system applicable not only to mice but also to rats and monkeys, thus advancing electrophysiological studies.

CRediT authorship contribution statement

Shinnosuke Idogawa: Conceptualization, Methodology, Investigation, Writing - original draft, Writing - review & editing. **Koji Yamashita:** Methodology, Investigation. **Rioki Sanda:** Methodology. **Rika Numano:** Writing - original draft, Writing - review & editing. **Kowa Koida:** Writing - original draft, Writing - review & editing. **Takeshi Kawano:** Supervision, Writing - original draft, Writing - review & editing, Funding acquisition.

Declaration of Competing Interest

The authors report no declarations of interest.

Acknowledgements

This work was supported by JSPS KAKENHI [grant numbers 17H03250, 26709024, and 20H00244]; and Strategic Advancement of Multi-Purpose Ultra-Human Robot and Artificial Intelligence Technologies program from NEDO, and Nagai Foundation for Science & Technology. R.N. was supported by Takeda Science Foundation. K.K. was supported by JSPS KAKENHI [grant number 15H05917].

Appendix A. Supplementary data

Supplementary material related to this article can be found, in the online version, at doi:https://doi.org/10.1016/j.snb.2020.129423.

References

[1] T.D. Yoshida Kozai, N.B. Langhals, P.R. Patel, X. Deng, H. Zhang, K.L. Smith, J. Lahann, N.A. Kotov, D.R. Kipke, Ultrasmall implantable composite microelectrodes with bioactive surfaces for chronic neural interfaces, Nat. Mater. 11 (2012) 1065–1073, https://doi.org/10.1038/nmat3468.
[2] L. Luan, X. Wei, Z. Zhao, J.J. Siegel, O. Potnis, C.A. Tuppen, S. Lin, S. Kazmi, R. A. Fowler, S. Holloway, A.K. Dunn, R.A. Chitwood, C. Xie, Ultraflexible nanoelectronic probes form reliable, glial scar–free neural integration, Sci. Adv. 3 (2017) 1–10, https://doi.org/10.1126/sciadv.1601966.
[3] C. Mora Lopez, J. Putzeys, B.C. Raducanu, M. Ballini, S. Wang, A. Andrei, V. Rochus, R. Vandebriel, S. Severi, C. Van Hoof, S. Musa, N. Van Helleputte, R. F. Yazicioglu, S. Mitra, A neural probe with up to 966 electrodes and up to 384 configurable channels in 0.13 μm SOI CMOS, IEEE Trans. Biomed. Circuits Syst. 11 (2017) 510–522, https://doi.org/10.1109/TBCAS.2016.2646901.
[4] K.E. Jones, P.K. Campbell, R.A. Normann, A glass/silicon composite intracortical electrode array, Ann. Biomed. Eng. 20 (1992) 423–437, https://doi.org/10.1007/BF02368134.
[5] A. Fujishiro, H. Kaneko, T. Kawashima, M. Ishida, T. Kawano, In vivo neuronal action potential recordings via three-dimensional microscale needle-electrode arrays, Sci. Rep. 4 (2014) 1–9, https://doi.org/10.1038/srep04868.
[6] G. Buzsáki, Large-scale recording of neuronal ensembles, Nat. Neurosci. 7 (2004) 446–451, https://doi.org/10.1038/nn1233.
[7] R.R. Harrison, P.T. Watkins, R.J. Kier, R.O. Lovejoy, D.J. Black, B. Greger, F. Solzbacher, A low-power integrated circuit for a wireless 100-electrode neural recording system, IEEE J. Solid-State Circuits 42 (2007) 123–133, https://doi.org/10.1109/JSSC.2006.886567.

[8] D. Fan, D. Rich, T. Holtzman, P. Ruther, J.W. Dalley, A. Lopez, M.A. Rossi, J. W. Barter, D. Salas-Meza, S. Herwik, T. Holzhammer, J. Morizio, H.H. Yin, A wireless multi-channel recording system for freely behaving mice and rats, PLoS One 6 (2011), https://doi.org/10.1371/journal.pone.0022033.
[9] T.A. Szuts, V. Fadeyev, S. Kachiguine, A. Sher, M.V. Grivich, M. Agrochão, P. Hottowy, W. Dabrowski, E.V. Lubenov, A.G. Siapas, N. Uchida, A.M. Litke, M. Meister, A wireless multi-channel neural amplifier for freely moving animals, Nat. Neurosci. 14 (2011) 263–270, https://doi.org/10.1038/nn.2730.
[10] R.R. Harrison, R.J. Kier, C.A. Chestek, V. Gilja, P. Nuyujukian, S. Ryu, B. Greger, F. Solzbacher, K.V. Shenoy, Wireless neural recording with single low-power integrated circuit, IEEE Trans. Neural Syst. Rehabil. Eng. 17 (2009) 322–329, https://doi.org/10.1109/TNSRE.2009.2023298.
[11] R.R. Harrison, H. Fotowat, R. Chan, R.J. Kier, R. Olberg, A. Leonardo, F. Gabbiani, Wireless neural/EMG telemetry systems for small freely moving animals, IEEE Trans. Biomed. Circuits Syst. 5 (2011) 103–111, https://doi.org/10.1109/TBCAS.2011.2131140.
[12] K. Abdelhalim, H.M. Jafari, L. Kokarovtseva, J.L.P. Velazquez, R. Genov, 64-Channel uwb wireless neural vector analyzer soc with a closed-loop phase synchrony-triggered neurostimulator, IEEE J. SolidState Circuits 48 (2013) 2494–2510, https://doi.org/10.1109/JSSC.2013.2272952.
[13] M. Yin, D.A. Borton, J. Komar, N. Agha, Y. Lu, H. Li, J. Laurens, Y. Lang, Q. Li, C. Bull, L. Larson, D. Rosler, E. Bezard, G. Courtine, A.V. Nurmikko, Wireless neurosensor for full-spectrum electrophysiology recordings during free behavior, Neuron 84 (2014) 1170–1182, https://doi.org/10.1016/j.neuron.2014.11.010.
[14] A. Zhou, S.R. Santacruz, B.C. Johnson, G. Alexandrov, A. Moin, F.L. Burghardt, J. M. Rabaey, J.M. Carmena, R. Muller, A wireless and artefact-free 128-channel neuromodulation device for closed-loop stimulation and recording in non-human primates, Nat. Biomed. Eng. 3 (2019) 15–26, https://doi.org/10.1038/s41551-018-0323-x.
[15] C.A. Chestek, V. Gilja, P. Nuyujukian, R.J. Kier, F. Solzbacher, S.I. Ryu, R. R. Harrison, K.V. Shenoy, HermesC: low-power wireless neural recording system for freely moving primates, IEEE Trans. Neural Syst. Rehabil. Eng. 17 (2009) 330–338, https://doi.org/10.1109/TNSRE.2009.2023293.
[16] H. Miranda, V. Gilja, C.A. Chestek, K.V. Shenoy, T.H. Meng, HermesD: A high-rate long-range wireless transmission system for simultaneous multichannel neural recording applications, IEEE Trans. Biomed. Circuits Syst. 4 (2010) 181–191, https://doi.org/10.1109/TBCAS.2010.2044573.
[17] H. Gao, R.M. Walker, P. Nuyujukian, K.A.A. Makinwa, K.V. Shenoy, B. Murmann, T.H. Meng, HermesE: A 96-channel full data rate direct neural interface in 0.13 μm CMOS, IEEE J. Solid-State Circuits 47 (2012) 1043–1055, https://doi.org/10.1109/JSSC.2012.2185338.
[18] H. Sawahata, S. Yamagiwa, A. Moriya, T. Dong, H. Oi, Y. Ando, R. Numano, M. Ishida, K. Koida, T. Kawano, Single 5 μm diameter needle electrode block modules for unit recordings in vivo, Sci. Rep. 6 (2016) 1–12, https://doi.org/10.1038/srep35806.
[19] A. Ikedo, T. Kawashima, T. Kawano, M. Ishida, Vertically aligned silicon microwire arrays of various lengths by repeated selective vapor-liquid-solid growth of n-type silicon/n-type silicon, Appl. Phys. Lett. 95 (2009) 33502, https://doi.org/10.1063/1.3178556.
[20] S. Yagi, S. Yamagiwa, Y. Kubota, H. Sawahata, R. Numano, T. Imashioya, H. Oi, M. Ishida, T. Kawano, Dissolvable base scaffolds allow tissue penetration of high-aspect-ratio flexible microneedles, Adv. Healthc. Mater. 4 (2015) 1949–1955, https://doi.org/10.1002/adhm.201500305.
[21] G. Buzsáki, A. Draguhn, Neuronal oscillations in cortical networks, Sci. 304 (5679) (2004) 1926–1929, https://doi.org/10.1126/science.1099745.
[22] G. Paxinos, K. Franklin, Paxinos Franklin's Mouse Brain Stereotaxic Coord, 2012.
[23] T. Yasui, S. Yamagiwa, H. Sawahata, S. Idogawa, Y. Kubota, Y. Kita, K. Yamashita, R. Numano, K. Koida, T. Kawano, A magnetically assembled high-aspect-ratio needle electrode for recording neuronal activity, Adv. Healthc. Mater. 8 (2019) 1–8, https://doi.org/10.1002/adhm.201801081.
[24] S. Idogawa, K. Yamashita, Y. Kubota, H. Sawahata, R. Sanda, S. Yamagiwa, R. Numano, K. Koida, T. Kawano, Coaxial microneedle-electrode for multichannel and local-differential recordings of neuronal activity, Sens. Actuators, B Chem. 320 (2020) 128442, https://doi.org/10.1016/j.snb.2020.128442.
[25] Y. Kubota, S. Yamagiwa, H. Sawahata, S. Idogawa, S. Tsuruhara, R. Numano, K. Koida, M. Ishida, T. Kawano, Long nanoneedle-electrode devices for extracellular and intracellular recording in vivo, Sensors Actuators B Chem. 258 (2018) 1287–1294, https://doi.org/10.1016/j.snb.2017.11.152.
[26] K. Funayama, G. Minamisawa, N. Matsumoto, H. Ban, A.W. Chan, N. Matsuki, T. H. Murphy, Y. Ikegaya, Neocortical rebound depolarization enhances visual perception, PLoS Biol. 13 (2015) 1–25, https://doi.org/10.1371/journal.pbio.1002231.
[27] K. Funayama, N. Hagura, H. Ban, Y. Ikegaya, Functional organization of flash-induced V1 offline reactivation, J. Neurosci. 36 (2016) 11727–11738, https://doi.org/10.1523/JNEUROSCI.1575-16.2016.
[28] X. Liu, B. Subei, M. Zhang, A.G. Richardson, T.H. Lucas, J. Van Der Spiegel, The PennBMBI: a general purpose wireless brain-machine-brain interface system for unrestrained animals, Proc. - IEEE Int. Symp. Circuits Syst. (2014) 650–653, https://doi.org/10.1109/ISCAS.2014.6865219.
[29] T. Harimoto, K. Takei, T. Kawano, A. Ishihara, T. Kawashima, H. Kaneko, M. Ishida, S. Usui, Enlarged gold-tipped silicon microprobe arrays and signal compensation for multi-site electroretinogram recordings in the isolated carp retina, Biosens. Bioelectron. 26 (2011) 2368–2375, https://doi.org/10.1016/j.bios.2010.10.014.

Shinnosuke Idogawa completed his B.S. degree in 2016 and M.S. degree in 2018 from the Department of Electrical and Electronic Information Engineering, Toyohashi University of Technology, Japan. He is pursuing his Ph.D. from the Department of Electrical and Electronic Engineering, Toyohashi University of Technology, Japan.

Koji Yamashita completed his B.S. degree in 2017 and M.S. degree in 2019 from the Department of Electrical and Electronic Information Engineering, Toyohashi University of Technology, Japan. He is pursuing his Ph.D. from the Department of Electrical and Electronic Engineering, Toyohashi University of Technology, Japan.

Rioki Sanda completed his B.S.in 2019 from Department of Electrical and Electronic Information Engineering, Toyohashi University of Technology, Japan. He is pursuing his M. S. at the same institution.

Rika Numano completed her B.Sc. in 1996, M.Sc. in 1998, and Ph.D. in 2002, all from Faculty of Technology, University of Tokyo, Japan. She was a Postdoctoral Research Fellow (Japan Society for the Promotion of Science), Human Genome Center Institute of Medical Science, University of Tokyo, Japan between 2002 and2005, Postdoctoral Fellow (Japan Society for the Promotion of Science Postdoctoral fellowship for research abroad), Department of Molecular and Cell Biology, University of California Berkeley between 2005 and 2006, a researcher, Cell Function Dynamics, RIKEN between 2006 and 2007, a Researcher, ERATO Project, Japan Science and Technology Agency between 2007 and 2010 and Tenure-truck Associate professor, Electronics-Inspired Interdisciplinary Research Institute (EIIRIS),Toyohashi University of Technology, between 2010 and 2013. Currently, from 2013, she is working as an Associate professor, at Department of Environmental and Life Sciences, Toyohashi University of Technology, Japan.

Kowa Koida completed his Ph.D. degree, Interdisciplinary Graduate School of Science and Engineering, Tokyo Institute of Technology, Japan in 2000. He had been a Postdoctoral Research Fellow during 2000–2007 at National Institute for Physiological Sciences, Japan. During 2007–2010 he worked as an Assistant Professor at the same institution. He is working as an Associate professor, Department of Computer and Science and Engineering, Toyohashi University of Technology, Japan, and Electronics Inspired-Interdisciplinary Research Institute (EIIRIS) at the same University.

Takeshi Kawano completed his M.S. degree in 2001, Ph.D. degree in 2004, and between 2004 and 2005, he was a Postdoctoral Research Fellow at Department of Electrical and Electronic Engineering, Toyohashi University of Technology, Japan. During 2005–2007, he was a Postdoctoral Research Fellow (Japan Society for the Promotion of Science Postdoctoral fellowship for research abroad), Department of Mechanical Engineering, Berkeley Sensor and Actuator Center (BSAC), University of California Berkeley. During 2007–2010 was an Assistant Professor, Toyohashi University of Technology, Electrical and Electronic Engineering, Japan. From 2010 on wards he has been PRESTO Researcher, Japan Science and Technology Agency (JST) as well as an Associate Professor, Electrical and Electronic Information Engineering Toyohashi University of Technology, Japan.